Drug Development and Industrial Pharmacy, 32:347–355, 2006

ISSN: 0363-9045 print / 1520-5762 online
DOI: 10.1080/03639040500519136

Taylor & Francis
Taylor & Francis Group

Continuous Grinding Kinetics of Ethenzamide Particles by Fluidized-Bed Jet-Milling

T. Fukunaka
Banyu Pharmaceutical Co., LTD., Okazaki, Aichi, Japan

B. Golman and K. Shinohara
Division of Chemical Process Engineering, Graduate School of Engineering, Hokkaido University, Sapporo, Hokkaido, Japan

ABSTRACT Continuous grinding kinetics of Ethenzamide powder, as a model active pharmaceutical ingredient (API) was investigated by fluidized-bed jet-milling. Because the oversize fractions after the classification were well fitted by a modified Rosin-Rammler distribution function, an equation of grade efficiency curve was obtained, which was also characteristic of API. A continuous grinding model was developed on the basis of a batch model by using 1st Kapur function relating grinding rate, the grade efficiency curve, and the overall process flow model consisting of grinding, classification, and mixing zones. The residual ratio obtained was well fitted to the experimental results except for the particle size range smaller than 4 μm and larger than 100 μm. Furthermore, because the volume of the active grinding zone adopted as the fitting parameter was found to be 5 cm^3 in all experiments and the value was considered to be appropriate dimensionally, this result supports the reliability of the model.

KEYWORDS Fluidized-bed jet-mill, Kinetics, Continuous grinding, Mathematical model, Ethenzamide

INTRODUCTION

In pharmaceutical field, a fluidized-bed jet-mill is relatively new equipment compared with the conventional ones such as a jet-mill and a pin-mill. Thus, the grinding kinetics have not fully been studied yet for API. Furthermore, because continuous operation is popular in industrial production, it is desirable to develop a continuous grinding model for the purpose of selection of optimum conditions.

For the continuous grinding by means of the fluidized-bed jet-mill, some studies have been carried out by using lactose and limestone. (Heng, P.W.S., et al., 2000; Chan, L. W., et al., 2002). However, they have mainly focused on the grinding characteristics qualitatively and not on the kinetics quantitatively. In addition, although Berthiaux et al. (1999) investigated the kinetics using alumina hydrate, the kinetics of API milling has not been studied yet.

The object of this article is to develop a continuous grinding model of fluidized-bed jet-milling with a model API, Ethenzamide particles, based on the batch model.

Address correspondence to T. Fukunaka, Banyu Pharmaceutical Co., LTD., 91, Kamimutsuna 3- chome, Okazaki, Aichi, 444-0858, Japan; Fax: +81-564-57-1766; E-mail: tadashi_fukunaka@merck.com (T. Fukunaka).

FUNDAMENTAL THEORY

Because the fluidized-bed jet-mill includes a mechanical classifier at the upper part of a chamber, the overall process is considered to correspond to a closed grinding circuit. Thus, the process flow diagram is shown in Fig. 1, where $R_0(x)$, $R(x)$ denote the oversize fractions of the feed and the product, and Q and M are the mass flow rates of the feed (or product) and the internal loop, respectively. Here, subscripts *i, e*, and *r* indicate the corresponding quantity at the inlet, the outlet of the grinding zone, and in the recycle loop, respectively. Practically, because it is impossible to measure the oversize fractions and the mass flow rates in the internal loop, it is necessary to calculate the material balances around the overall process to obtain the relationships between these unknown variables and $R_0(x)$, $R(x)$, and Q, which can be measured.

Grinding Zone

In the case of short grinding time, based on a Kapur model (1970) for batch grinding, Berthiaux and Dodds (1999) developed a simplified equation based on the variation of a residual ratio, $f(x,t)$ with time. It is defined as the ratio of oversize fraction at time *t*, $R(x,t)$ to initial one, $R(x,0)$ to characterize the proportion of particles not to be subjected to the batch grinding action at time *t*:

$$f(x,t) = \frac{R(x,t)}{R(x,0)} = \exp[K^{(1)}(x)t] \tag{1}$$

Here the terms in the square bracket is called the "first Kapur function" which includes the complicated breakage and selection functions. The opposite sign of the function can express the selection function. (Berthiaux, H., et al., 1996).

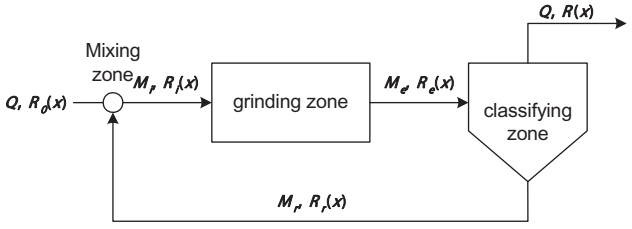

FIGURE 1 **Flow diagram of overall process with fluidized-bed jet-mill.**

For the continuous grinding system, Berthiaux et al. (1999) proposed the following equation considering the residence time distribution, *E(t)* of the particle in the grinding zone:

$$f(x) = \frac{R_e(x)}{R_i(x)} = \int_0^\infty f(x,t)E(t)dt \tag{2}$$

Assuming the perfect mixing state in this zone, the residence time distribution is expressed as:

$$E(t) = \frac{e^{-t/\tau}}{\tau} \tag{3}$$

where τ is the space time given by the holdup divided by the feed rate.
Substitution of Eqs. (1) and (3) into Eq. (2) gives the following:

$$f(x) = \frac{1}{1-\tau\{K^{(1)}(x)\}} \tag{4}$$

Classifying Zone

To characterize the classification performance of the mill, the grade efficiency curve, $\Gamma(x)$ was calculated by using the material balance around the classifier as follows:

$$\frac{1}{\Gamma(x)} = 1 + \left[\frac{1}{E_T} + 1\right]\frac{dR}{dR_r} \tag{5}$$

where E_T is the total efficiency defined as:

$$E_T = \frac{M_r}{M_e} \tag{6}$$

Because the grade efficiency curve frequently does not go through the origin due to the imperfect separation, a reduced grade efficiency curve, $\Gamma_r(x)$ is defined as:

$$\Gamma_r(x) = \frac{\Gamma(x) - \Gamma_d}{1 - \Gamma_d} \tag{7}$$

where Γ_d is the dead flux of grade efficiency corresponding to the amount of fine particles below a certain size which can be carried along with the grinding gas, as $\Gamma(0)$.

In the case that the oversize fraction can be expressed by the following Rosin-Rammler distribution function [Eq. (8)], Eq. (5) is rewritten as (Berthiaux et al., 1999):

$$R(x) = \exp[-(x/x_p)^n] \tag{8}$$

$$\Gamma(x) = \frac{1}{1+\frac{n_f}{n_c}\left[\frac{1}{\varepsilon_T}-1\right]\left[\frac{x_{p_c}}{x_{p_f}}\right]x^{n_f-n_c}\exp\left[\left[\frac{x}{x_{p_c}}\right]^{n_c}-\left[\frac{x}{x_{p_f}}\right]^{n_f}\right]} \tag{9}$$

Here, x_p is the absolute size constant, n is the distribution constant, and subscripts f and c denote the fine and the coarse fractions, respectively. ε_T is the total efficiency of separation in the classification experiment. It is analogous to E_T and E_{Tr} in the continuous grinding experiment.

Analysis of Continuous Grinding Model

Material balances around each zone shown in Fig. 1 can be expressed as:

$$\text{Mixing zone:} \quad M_i R_i(x) = M_r R_r(x) + Q R_0(x) \tag{10}$$

$$\text{Grinding zone:} \quad R_e(x) = f(x)\, R_i(x) \tag{11}$$

$$\text{Classifier zone:} \quad M_e R_e(x) = M_r R_r(x) + Q R(x) \tag{12}$$

By combining Eqs. (10–12) with Eq. (5), it is possible to define a residual ratio corresponding to the continuous grinding process using the measurable variables as $R_0(x)$ and $R(x)$:

$$f_{proc}(x) = \frac{R(x)}{R_0(x)} = \frac{1}{\frac{1}{f(x)}+\frac{1}{R(x)}\left[\frac{1-f(x)}{f(x)}\right]\int_0^x\left[\frac{\Gamma(x)}{1-\Gamma(x)}\right]\frac{dR}{dx}dx+\frac{E_T}{1-E_T}} \tag{13}$$

In the case of the classifier with dead flux, Eq. (13) can be rewritten by replacing E_T and $\Gamma(x)$ with the reduced quantities E_{Tr} and $\Gamma_r(x)$, respectively, and the reduced total efficiency of the classifier in the overall process, E_{Tr} is expressed as:

$$E_{Tr} = \frac{\int_0^\infty \frac{\Gamma_r(x)}{1-\Gamma_r(x)}\frac{dR}{dx}dx}{\int_0^\infty \frac{\Gamma_r(x)}{1-\Gamma_r(x)}\frac{dR}{dx}dx - 1} \tag{14}$$

To link the space time, τ in Eq. (3) to E_{Tr}, the active volume, V inside the mill is defined as a fitting parameter (Berthiaux, et al., 1999):

$$\tau = \frac{\rho V}{Q}(1-E_{Tr}) \tag{15}$$

where ρ is the solid density.

EXPERIMENTAL

Materials

Ethenzamide particles ($C_9H_{11}NO_2$: MW 165.19, 1.25 g/cm^3, initial particle size: 55.4 μm, IWAKI SEIYAKU Co., Ltd.), which are needle-shaped and highly cohesive, were used as a raw material.

Methods

Grinding and Classifying Equipment

The fluidized-bed jet-mill (HOSOKAWA MICRON Corp. Counter Jet-mill 100 AFG) was used in the series of experiments, as schematically shown in Fig. 2. The grinding chamber consists of a cylindrical part with 97.4 mm inside diameter and a conical bottom, and the total volume is 950 cm^3. Three grinding nozzles of 1.9 mm in opening diameter are located horizontally at 120° intervals in the bottom at about 162 mm from the center of the classifier rotor. The raw material was fed into the chamber from the top with a screw feeder, and is accelerated by nitrogen gas compressed up to 0.60 MPa from the nozzles to meet at the same point. The milled particles are classified by 50 ATP turbo-selector (50 mm outside diameter, maximum rotor speed: 22000 rpm), which is located above the chamber. The classified fine particles leaving the chamber are collected as a product in a bag-filter. The rejected coarse particles are recirculated in the

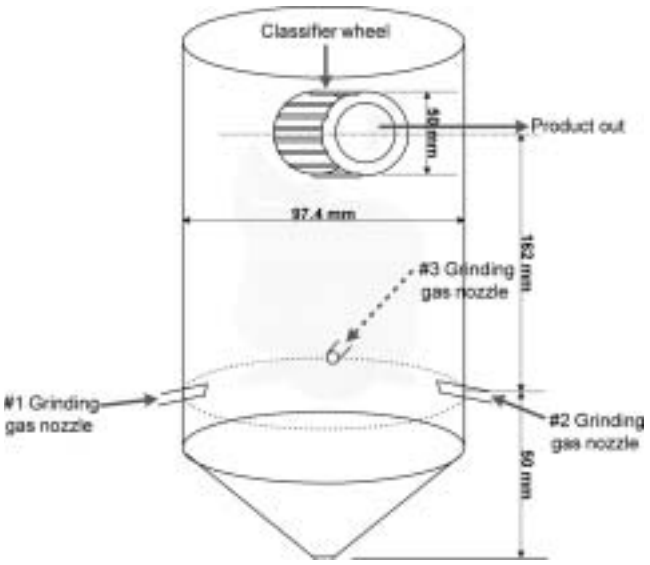

FIGURE 2 **Schematic illustration of fluidized-bed jet-mill.**

chamber until they are ground into size smaller than a critical size to pass through the classifier rotor. The nitrogen passed through the filter is vented to atmosphere by a blower via HEPA filter. Figure 3 shows the schematic diagram of the experimental setup. The switchover between grinding and classifying operations was made by exchanging two types of bottom chambers (#9 and #10, respectively). The classifying chamber consists of a conical bottom with a louver for gas distribution and an elbow piping with three nozzles for drawing the gas to the louver which is set circumferentially. In both the grinding and the classifying experiments, the same nozzles were used to keep the same gas flow rate.

Continuous Grinding Experiment

Particles at given feed rate were fed continuously into the chamber from the top with the screw feeder, and the classifier is set to a given speed of rotation to keep the constant holdup of particles inside the mill. Product particles leaving the chamber were collected in the outside cyclone. The equipment was operated under the same blower control as in the batch experiment by keeping the pressure inside the mill –0.3 kPa. Experiments (Runs #1 and #2) were carried out at the feed rate of 0.5 kg/h, the grinding pressure of 0.4 MPa corresponding to the gas flow rate of 30.6 m^3/h, and the classifier rotor speeds of 8500 and 8750 rpm, respectively.

Classifying Experiment

The feed material is dispersed and distributed by nitrogen gas passing though the louver. The classified particles leaving the grinding chamber are collected as "fine" with a cyclone. The remained particles in the chamber are collected as "coarse" component in the pot.

The gas flow rate was kept the same as that of the continuous grinding experiments by setting the same gas pressure. The feed material was prepared by mixing premilled fine particles and preclassified coarse

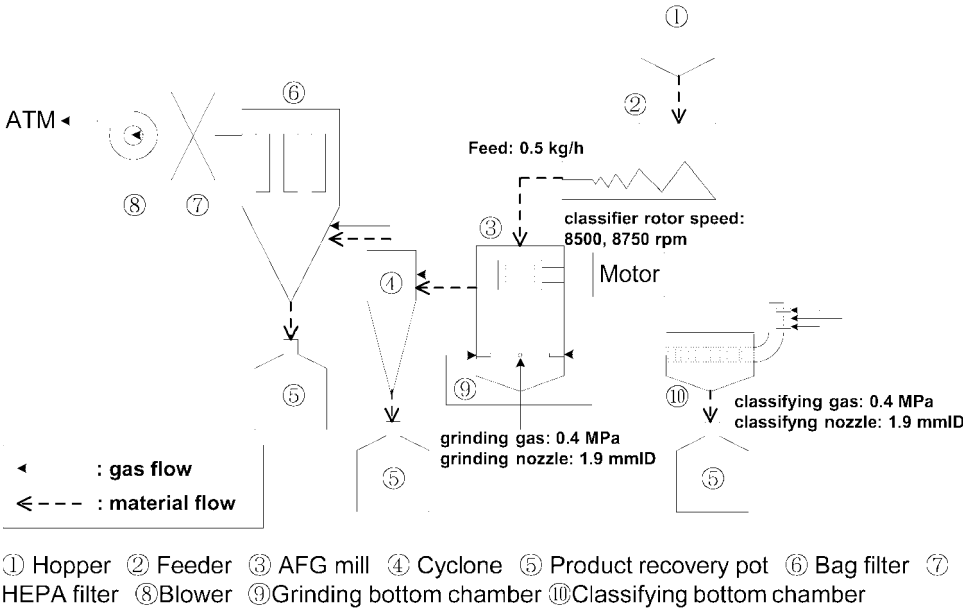

FIGURE 3 **Experimental setup of fluidized-bed jet-mill.**

ones in a roughly 50–50% split. The feed rate was the same as in the continuous grinding one. Experiments (Runs #3 and #4) were carried out at the classifier rotor speeds of 8500 and 8750 rpm, respectively.

Particle Size Distribution

The particle size distribution was measured by means of a wet-type laser diffraction analyzer (MICROTRACK HRA Model#6320-X100, NIKKISO Co., Ltd). The sample was set up by suspending particles in the 10 mL of the mixture of isoparaffinic hydrocarbons (Isopar-G, ExxonMobil Chemical) with 0.25 wt% lecithin (Wako Pure Chemical Industries, Ltd.) as a dispersant and measured under deaggregation condition after sonication.

RESULTS AND DISCUSSION

Determination of Classifier Rotor Speed

To make the holdup inside the mill 50 or 80 g corresponding to the same amounts in the batch grinding experiments, continuous grinding was carried out to determine the classifier rotor speed required. Figure 4 shows the historical data of the holdup at two rotor speeds. It was found that at the speeds of 8500 and 8750 rpm, the times required to reach the steady state were 30 and 40 min, respectively, and they were suitable for 50 and 80 g of holdup, respectively. Figure 5 also shows the variation of the volumetric mean particle size inside the mill for two rotor speeds. As the time went on, the mean size decreased gradually and

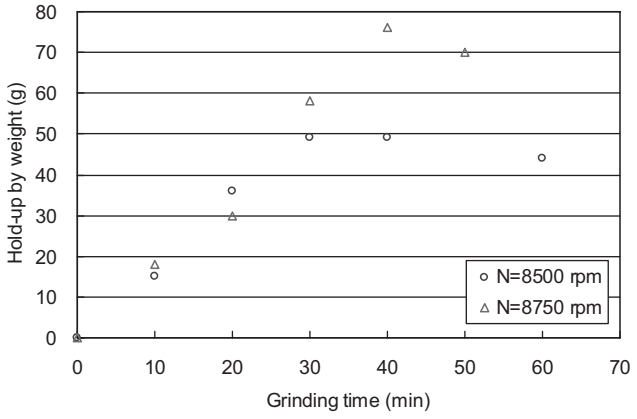

FIGURE 4 **Historical data of holdup inside mill at two rotor speeds.**

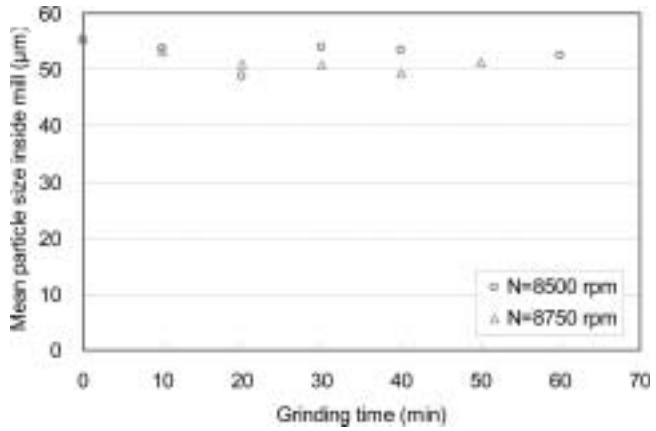

FIGURE 5 **Variation of volumetric mean particle size inside a mill chamber.**

reached about 50 μm at the steady state. There were no significant differences in particle size within the mill between Runs #1 and #2, because the values of the rotor speed were close. However, a difference was observed in the mean sizes of milled particles collected in the product recovery pot with higher rotor speed resulting in the smaller particles. The oversize fractions of collected particles in the cyclone together with raw material are shown in Figure 6. The mean particle size at 8750 and 8500 rpm reduces from 55.4 to 23.1 and 27.3 μm as a result of grinding, respectively.

Determination of Grade Efficiency Curve

The grade efficiency curve was determined from the classification experiments (Runs #3 and #4). Figure 7a

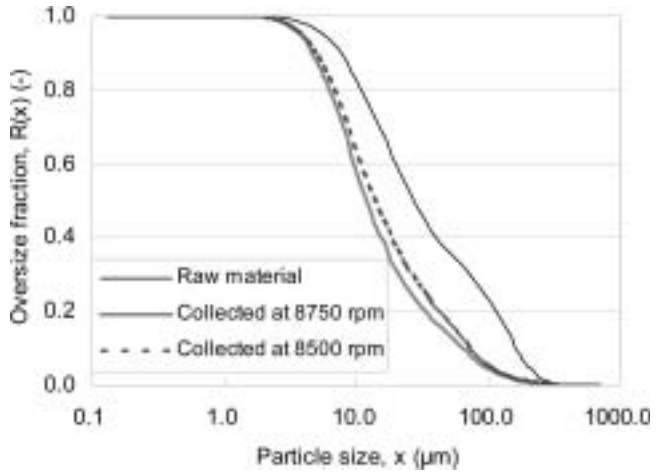

FIGURE 6 **Oversize fractions of particles collected in cyclone at two speeds and raw material.**

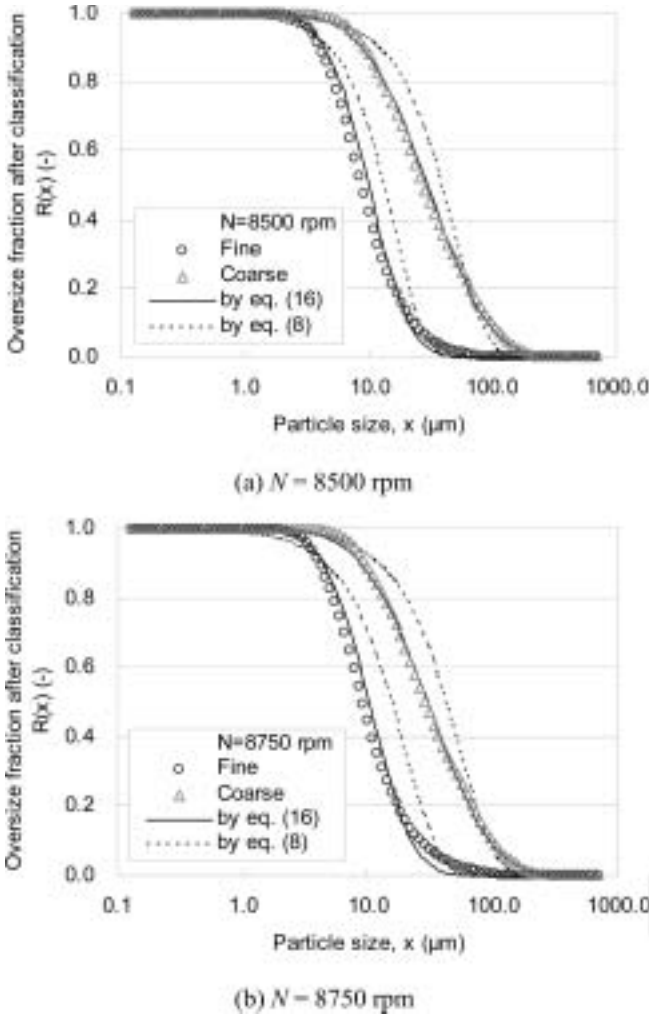

FIGURE 7 **Oversize fractions of classified fine and coarse particles at two rotor speeds.**

and b show the oversize fractions of the classified fine and coarse particles at two rotor speeds. The dashed lines in the graphs indicate the calculated lines by Rosin-Rammler distribution, but they were not suitable for the experimental data of API. Therefore, we propose a modified distribution as:

$$R(x) = \exp[-B\{\ln(x)\}^A] \tag{16}$$

where A and B are experimental parameters, as listed in Table 1.

The experimental data are well fitted by Eq. (16). It is considered that the proposed equation is suitable for representing the oversize fraction of API, because it focuses on a smaller particle size range than Rosin-Rammler distribution.

TABLE 1 **Results of Classifying Experiments**

	N = 8500 rpm		N = 8750 rpm	
	Fine	Coarse	Fine	Coarse
A	4.2453	4.2528	4.1404	4.1590
B	1.9901E-02	3.8048E-03	2.0630E-02	4.2209E-03
ε_T	0.638		0.587	
E_{Tr}	0.880		0.894	
Γ_d	0.2482		0.2172	

Hence, differentiations of R relative to size x are given as:

$$\frac{dR(x)}{dx} = \frac{-AB\exp[-B\{\ln(x)\}^A]\{\ln(x)\}^{A-1}}{x} \tag{17}$$

Substitution of these equations for coarse and fine fractions into equation (5) leads to:

$$\Gamma(x) = \frac{1}{1+\left[\frac{1}{\varepsilon_T}-1\right]\{\ln(x)\}^{A_f-A_c}\left(\frac{A_fB_f}{A_cB_c}\right)\exp\left[B_c\{\ln(x)\}^{A_c}-B_f\{\ln(x)\}^{A_f}\right]} \tag{18}$$

Figure 8a and b show the grade efficiency and the reduced grade efficiency curves at two rotor speeds. The characteristic parameters for each curve are also presented in Table 1. Although these curves were almost consistent with each other due to the narrow operational range, the efficiency, ε_T at lower speed was slightly higher than the value at higher speed. This may have been due to small differences in feed particle size distribution among experiments, e.g., if the feed material prepared by mixing the fine and the coarse particles was not uniform due to segregation during operations.

Development and Evaluation of Continuous Grinding Model

To develop a continuous grinding model for the fluidized-bed jet-mill, product samples collected in the continuous experiments (Runs #1 and #2) were used. Figure 9 shows the oversize fractions of products at two rotor speeds. Although these curves were almost

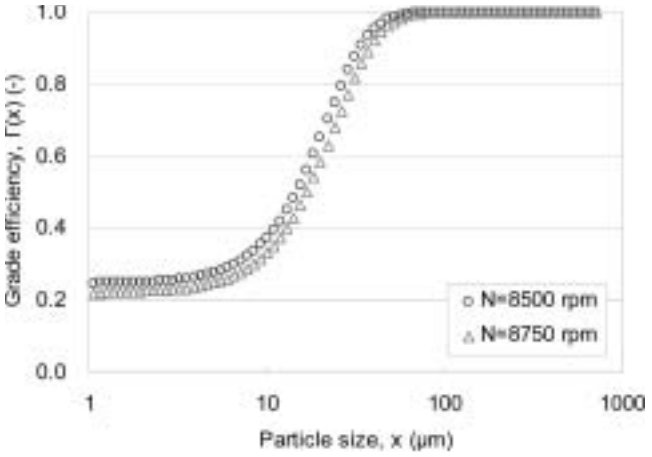

(a) Grade efficiency curves by equation (18)

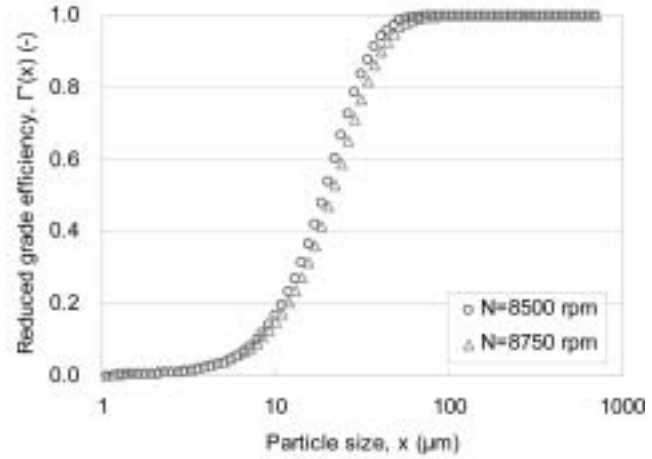

(b) Reduced grade efficiency curves by equation (7)

FIGURE 8 **Grade efficiency and reduced grade efficiency curves at two rotor speeds.**

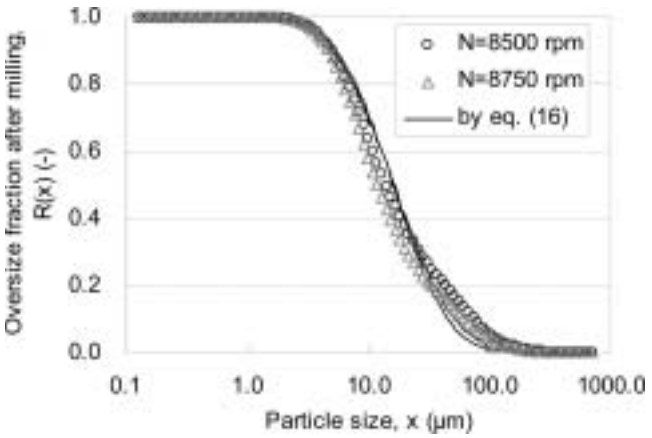

FIGURE 9 **Oversize fractions of products in continuous grinding at two rotor speeds.**

consistent with each other, the fraction at higher speed was a little bit sharper than that at lower one. This is the opposite of the results in the classifying experiments, which is hypothesized to be due to a difference in grinding ability which is caused by the mill holdup, as observed in the batch grinding experiment. These curves were also fitted by Eq. (16), and the corresponding parameters were given in Table 2.

The residual ratio for continuous grinding was determined analytically from Eq. (13) using the milled oversize fraction by Eq. (16), the volume of active grinding zone by Eq. (15) as the fitting parameter, the residual ratio by Eq. (4), the reduced grade efficiency curve by Eqs. (7) and (18), and the reduced total efficiency by Eq. (14). The 1st Kapur function in Eq. (4) was obtained by fitting data from the batch experiment with the following equation:

$$K^{(1)}(x) = a(\ln(x))^3 + b(\ln(x))^2 + c(\ln(x)) + d \qquad (19)$$

Figure 10 (a) and (b) show the fit of the continuous grinding data by Eq. (13) at two rotor speeds. It was found that calculated line using a value of 5 cm^3 for net solid volume in the active grinding zone was most suitable for the experimental data. The results are considered to be appropriate dimensionally, because "gross" active grinding zones considering the bed density at 8500 and 8750 rpm are 119 and 74 cm^3, respectively. These volumes are equivalent to the volume of spheres of 6.1 and 5.2 cm in diameter, respectively. For the particle size range smaller than 4 μm, Eq. (13) could not be used for fitting of the experimental data. This is because the functional form of Eq. (19) uses the logarithm of particle size in the batch grinding. The discrepancy between the calculated values and the experimental data for particles larger than 100 μm is considered to be caused by the carryover of coarse particles in the continuous grinding due to the local jet stream from the grinding nozzles. Figure 11 (a) and (b) show the comparison of oversize fractions of products obtained by continuous grinding and classifying experiments at two rotor speeds. It is found that the size distributions of products of grinding are broader than those produced by classification due to the existence of particles larger than 100 μm at both rotor

TABLE 2 **Results of Continuous Grinding Experiments**

N	8500 rpm	8750 rpm
A	3.8046	3.4761
B	1.4025E-02	1.9320E-02

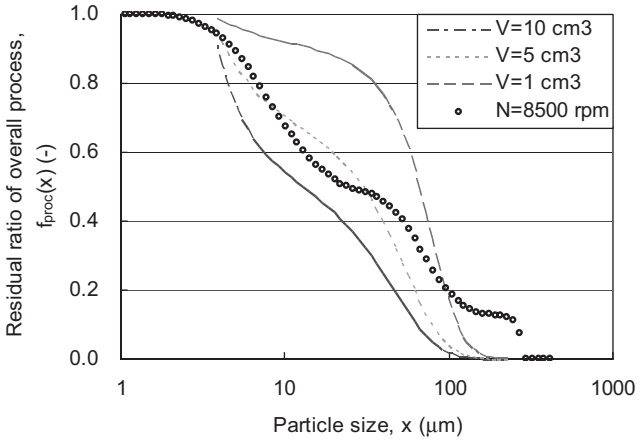

(a) N = 8500 rpm

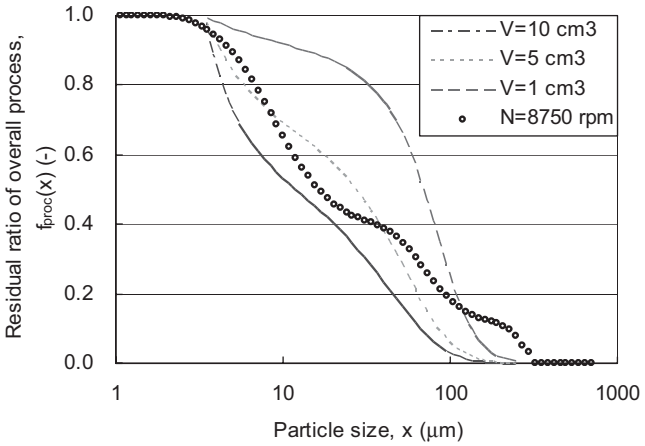

(b) N = 8750 rpm

FIGURE 10 **Fitting of continuous grinding data by Eq. (13) at two rotor speeds.**

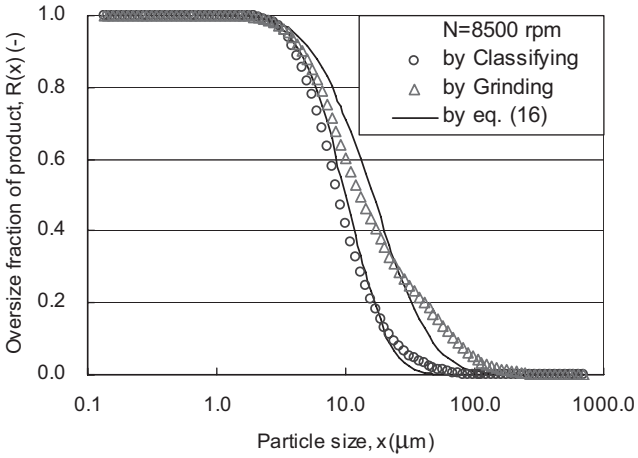

(a) N = 8500 rpm

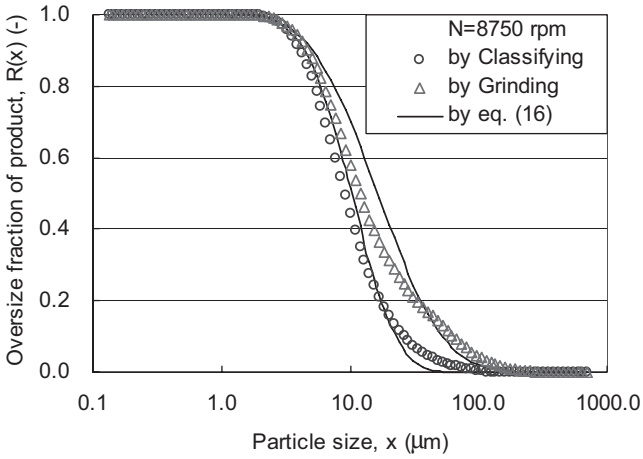

(b) N = 8750 rpm

FIGURE 11 **Comparison of oversize fractions of products obtained by continuous grinding and classifying experiments at two rotor speeds.**

speeds, at the same operating conditions. However, despite the difficulty in handling due to the characteristics of APIs, which are fine and highly cohesive, and the complexity of the shape of the oversize fraction, the developed model of the continuous grinding in general successfully expresses the residual ratio of API by fluidized-bed jet-milling.

CONCLUSION

Continuous grinding kinetics of Ethenzamide powder was investigated by fluidized-bed jet-milling as a typical sample of an active pharmaceutical ingredient. As a result, the following findings were made:

1. In the classification experiments, the oversize fractions for classified fine and coarse particles were well fitted by the modified Rosin-Rammler distribution function. The equation of grade efficiency curve obtained was characteristic for API.
2. In the continuous grinding experiments, although the oversize fractions for products were also well fitted by the modified Rosin-Rammler distribution, they were broader than that by independent classification experiments at the same condition. This is presumed to be caused by the carryover of coarse particles due to the local jet stream from the grinding nozzles.
3. The continuous grinding model corresponding to closed grinding circuit was developed and well expressed the experimental residual ratio obtained except for particle sizes smaller than 4 μm and larger than 100 μm.
4. The active grinding zone adopted as the fitting parameter was 5 cm^3 on net volume of particles, which was appropriate dimensionally in all the experiments.

NOMENCLATURE

A, B	Coefficients in Eq. (16)	
a, b, c, d	Coefficients and constant in Eq. (19)	
E	Residence time distribution of particles in grinding zone	(1/s)
E_T	Total efficiency of classifier in overall process	
E_{Tr}	Reduced total efficiency of classifier in overall process	
f	Residual ratio related to grinding zone	
f_{proc}	Residual ratio related to overall process	
$K^{(1)}(x)$	1st-order Kapur function	(1/s)
M	Mass flow rate in internal loop	(kg/h)
n	Distribution constant	
Q	Mass flow rate of solids feed	(kg/h)
R	Oversize fraction	
t	Grinding time	(s)
x	Particle sizes	(μm)
x_p	Absolute size constant	(μm)
V	Volume of active grinding zone	(m^3)
Γ	Grade efficiency of classifier	
Γ_r	Reduced grade efficiency of classifier	
ε_T	Total efficiency in classifying experiment	
ρ	Solid density	(kg/m^3)
Γ_d	Dead flux of grade efficiency	
τ	Space time	(s)

Subscripts

c	Coarse particles remaining inside mill in classification experiment
e	Outlet of grinding zone
f	Fine particles leaving mill in classification experiment
i	Inlet of grinding zone
r	Recycle loop
0	Feed

REFERENCES

Berthiaux, H., Chiron, C., & Dodds, J. (1999). Modeling fine grinding in a fluidized bed opposed jet mill. II: Continuous grinding. *Powder Technol.*, *106*, 88–97.

Berthiaux, H., & Dodds, J. (1999). Modeling fine grinding in a fluidized bed opposed jet mill. I. Batch grinding kinetics. *Powder Technol.*, *106*, 78–87.

Berthiaux, H., Varinot, C., & Dodds, J. (1996). Approximate calculation of breakage parameters from batch grinding tests. *Chem. Eng. Sci.*, *51*, 4509–4516.

Chan, L. W., Lee, C. C., & Heng, P. W. S. (2002). Ultrafine grinding using a fluidized bed opposed jet mill: Effects of feed load and rotational speed of classifier wheel on particle shape. *Drug Dev. Ind. Pharm.*, *28*, 939–947.

Heng, P. W. S., Chan, L. W., & Lee, C. C. (2000). Ultrafine grinding using a fluidized bed opposed jet mill: effects of process parameters on the size distribution of milled particles. *Journal of Pharmaceutical Sciences*, *10*, 445–451.

Kapur, P. C. (1970). Kinetics of batch grinding. Part B. An approximate solution to the grinding equation. *Trans. Soc. Min. Eng. AIME.*, *247*, 309–313.